In-situ Formation and Assembly of Gold Nanoparticles by Gum Arabic as Efficient Photothermal Agent for Killing Cancer Cells[a]

Ching-Ping Liu, Fong-Sian Lin, Chih-Te Chien, Sheng-Yang Tseng, Chih-Wei Luo, Chien-Hung Chen, Jen-Kun Chen, Fan-Gang Tseng, Yeukuang Hwu, Leu-Wei Lo, Chung-Shi Yang, Shu-Yi Lin*

Gold nanoparticles (AuNPs) have been established to sufficiently eradicate tumors by means of heat production for photothermal therapy. However, the translation of the AuNPs from bench to the clinic still remains to be solved until realizing high bioclearance after treatment. Herein, we developed a simple strategy for simultaneous formation and assembly of small-size gold nanoparticles (Au-SNPs) to form a novel nanocomposite in the presence of gum arabic (GA) by synchrotron X-ray irradiation in an aqueous solution within 5 min. GA, a porous polysaccharide, can not only provide a confined space in which to produce uniform Au-SNPs (1.6 ± 0.7 nm in diameter), but can also facilitate the formation of Au-SNPs@GA (diameter $\approx$ 40 nm) after irradiating synchrotron X-rays. Specifically, the Au-SNPs@GA possesses high thermal stability and a strong photothermal effect for killing cancer cells. Importantly, a bioclearance study demonstrated that the Au-SNPs@GA can be gradually excreted by the renal and hepatobiliary system, which might be due to the breakdown and oxidation of GA under irradiating synchrotron X-rays. Thus, the novel gold nanocomposite can be promising photothermal agents for cancer treatment at the therapeutic level, minimizing toxicity concerns regarding long-term accumulation in vivo.

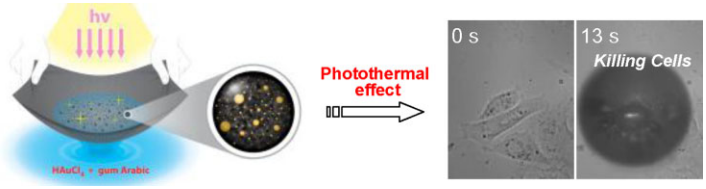

Dr. C.-P. Liu, F.-S. Lin, Dr. C.-T. Chien, C.-H. Chen, Dr. J.-K. Chen, Dr. L.-W. Lo, Dr. C.-S. Yang, Dr. S.-Y. Lin
Center for Nanomedicine Research, Division of Medical Engineering Research, National Health Research Institutes, 35 Keyan Road, Zhunan 35053, Taiwan
E-mail: shuyi@nhri.org.tw
Dr. S.-Y. Tseng, Dr. C.-W. Luo
Department of Electrophysics, National Chiao Tung University, Hsinchu 30010, Taiwan
F.-S. Lin, Dr. F.-G. Tseng, Dr. C.-S. Yang
Department of Engineering and System Science, National Tsing Hua University, Hsinchu 30013, Taiwan
Dr. Y. Hwu
Institute of Physics, Academia Sinica, Nankang Taipei 115, Taiwan

[a]**Supporting Information** is available from the Wiley Online Library or from the author.

1. Introduction

The photothermal effect of gold nanoparticles (AuNPs) has been found to increase medicinal benefits in therapeutic applications by eradicating tumors through heating.[1–6] However, this desirable utility in terms of medicinal purposes has been limited by an adverse effect in that AuNPs with a strong photothermal effect are not excretable.[7–9] AuNPs with dimensions of >5 nm (hereafter denoted as Au-LNPs) have strong photothermal effects, but tend to accumulate more in the liver[10–14] than AuNPs with dimensions of <5 nm (hereafter denoted as Au-SNPs) after intravenous administration.[12] After long-term accumulation in vivo, unpredictable

DOI: 10.1002/mabi.201300162

toxicity from Au-LNPs can become a big problem. In contrast, while Au-SNPs have been shown to be easily excreted by the renal clearance,[9,12] their photothermal effects are not efficient.[15] Recently, however, it has become possible to overcome the size-dependent limitations of photothermal effects by assembling Au-SNPs to form a supramolecular nanocomposite. Generally, a synthetic strategy can easily be achieved by manipulating a specific interaction between Au-SNPs and polymers.[1,16] Therefore, once the biosafety is established for intravenous injection, such excretable nanomaterials might become useful in clinical applications.

Gum Arabic (GA) is an edible polysaccharide and has been established as a protector to avoid aggregation of Au-LNPs, in which GA surrounds the surface of Au-LNPs (hereafter denoted as GA-protected Au-LNPs).[17,18] For example, Katti's group used alanine-based phosphine as a reducing agent to synthesize GA-protected Au-LNPs as a computer tomography (CT) contrast agent, as well as producing the radioactive ^{198}Au-LNPs for cancer therapy.[18–21] Additionally, Chen et al. used gold ion solutions and GA to synthesize GA-protected Au-LNPs through heating in the absence of reducing agents, and the resulting Au-LNPs were stable in high ionic strength solutions.[22] It has been known that the size of GA-protected AuNPs was typically 15–20 nm.[19] To the best of our knowledge, none of previous work reported AuNPs assembly synthesized by GA through any reduction methods. Recently, the supramolecular self-assembly approach[1] and hydrogels[23] have been extensively reported to synthesize various metal nanocomposites. However, there are few methods including in-situ reduction of metallic precursors,[24,25] and none of them deals with clearance in vivo.

Herein, we developed a simple strategy for simultaneous formation and assembly of Au-SNPs to form a new nanocomposite in the presence of GA by irradiating synchrotron X-rays (4–30 keV, 10^5 Gy s^{-1}). Synchrotron X-ray irradiation has been well established as a tool utilized in the formation of metallic nanoparticles.[26] In this work, GA and gold ions were added to a 5 mL aqueous solution, then the mixture was irradiated by synchrotron X-rays for approximately 5 min. After that, the nucleation and growth of gold ions were confined within the inherent porous structure of GA. In addition, the resulting Au-SNPs were trapped in GA to form an Au-SNPs@GA nanocomposite, preventing further aggregation of Au-SNPs or formation of Au-LNPs after reduction. Specifically, the resulting Au-SNPs@GA can be used as a new photothermal agent, which first exhibited a strong photothermal effect for killing cancer cells. The bioclearance study of the Au-SNPs@GA was also examined based on pharmacokinetics and biodistribution, demonstrating that the Au-SNPs@GA can be gradually excreted via the urinal system and hepatobiliary pathway.

2. Experimental Section

2.1. Preparation and Characterization of Au-SNPs@GA

AuNPs were synthesized in the presence or absence of GA at beam-line BL01A of the National Synchrotron Radiation Research Center (Hsinchu, Taiwan). GA and a 0.2% aqueous solution of $HAuCl_4$ were purchased from Sigma-Aldrich and used without further purification. For the synthesis of Au-SNPs@GA, 0.2–1 mL of $HAuCl_4$ solution and 1 mL of 4% (w/w) aqueous GA were mixed in 5 mL of deionized water (18 MΩ cm^{-1}). The reaction mixtures were irradiated with synchrotron X-rays (4–30 keV, 10^5 Gy s^{-1}) at room temperature for 5 min. No other chemical reducing agents or catalysts were used for any of the reactions. The Au-SNPs@GA were characterized by UV–vis spectroscopy (DU-800, Beckman Coulter), and transmission electron microscopy (H-7650, Hitachi). The surface plasmon band and the stability of the Au-SNPs@GA were analyzed using UV–vis spectroscopy in deionized water and a phosphate-buffered saline (PBS) solution containing 10% fetal bovine serum (FBS). (Note that arabinogalactan can be used to replace GA as a template for the Au-SNPs@GA synthesis.)

2.2. Analyses

Analyses methods are reported in the Supporting Information.

2.3. Micro-bubble Generation and the Photothermal Effect

The photothermal effect of Au-SNPs@GA was studied, using a 532 nm continuous wave (CW) laser (Coherent, Verdi-V10) to induce micro-bubble generation. The Au-SNPs@GA (6 mg mL^{-1}) was loaded onto glass slides and irradiated with the CW laser at 182.5 mW with a 10× objective lens, nominal aperture (NA) = 0.3. The micro-bubble formation upon laser irradiation of Au-SNPs@GA was observed with a homemade microscope system and then imaged on a charged coupled device (CCD) camera (MTV-12V1E; Mintron). For cell experiments, the surface of the Au-SNPs@GA was modified with polylysine to enhance intracellular uptake, and then cultured with breast cancer cells (MDA-MB-231) for 5 h. Excess Au-SNPs@GA were removed from the cultured cells, and then irradiated with a CW laser at 99.2 mW with a 40× objective lens (Plan FluorELWD; NA = 0.6, Nikon). Within the control groups, cells without treatment, or treatment with Au-SNPs@GA in the absence of polylysines, were given laser irradiation at a fixed power of 99.2 mW. All groups were run, with each experiment being repeated three times.

2.4. Evaluation of Pharmacokinetics and Biodistribution

Seven-week-old male ICR mice (25–30 g) were used for these studies. The mice used in this study were kept on a 12 h light/12 h dark cycle at 24 ± 2 °C and at 50 ± 10% relative humidity; water and food were available ad libitum. The mice were purchased from BioLASCO (Taipei, Taiwan) and transported in a temporary vivarium (an independently ventilated cage) to the Animal Molecular Imaging Core Facility at the National Health Research Institutes, where they were acclimated. On the day of the experiments, the mice were grouped into separate metabolism cages. Animals were handled in accordance with standard animal husbandry practices and regulations; they were treated humanely and with regard for alleviation of suffering throughout the study. Mice were anaesthetized with isoflurane, and suspensions of ^{198}Au-SNPs@GA were injected intravenously ($N = 3$) at a dose of 2.47 ± 0.16 μCi/mouse for biodistribution evaluation. The injection volume was 100 μL per mouse. The mice were euthanized with 100% CO_2 at 1 h, 4 h, 1 d, 2 d, 3 d, 6 d, and 7 d intervals after injection. Prior to euthanization, blood was collected from the retro-orbital plexus region in heparinized glass tubes. After the mice were sacrificed, their hearts, livers, lungs, spleens, kidneys, stomachs, pancreases, brains, intestines, and carcasses were collected, along with urine and feces. The tissues were briefly washed with normal saline and dried with blotting paper. Organs, urine, and feces were collected in a bottle and analyzed using a γ counter (2480 WIZARD2, PerkinElmer). The amounts of Au-SNPs@GA were determined from the radiation-count data, using a ^{198}Au half-life of 2.7 d.

3. Results and Discussion

3.1. Preparation and Characterization of Au-SNPs@GA

We prepared an Au-SNPs@GA nanocomposite by a simple approach, using intense X-ray irradiation in the co-existence of GA and gold ions. Transmission electron microscopy (TEM) images with negative staining (Figure 1a) show that the Au-SNPs@GA formed spherical shapes with diameters of approximately 40 nm. The fact that the presence of GA leads to the formation and assembly of Au-SNPs was proved by TEM images and their statistical analysis. The growth of Au-SNPs was well-controlled and had an average particle diameter of 1.6 ± 0.7 nm (Figure 1b). In contrast, Au-LNPs (10 to 80 nm in diameter) were dominant when a similar preparation was performed in the absence of GA (Supporting Information, Figure S1). Additionally, by simply adjusting the volume of 0.2% $HAuCl_4$ solution versus that of GA (40 mg mL^{-1}), we were able to obtain a size distribution of Au-SNPs@GA between 40 and 70 nm using dynamic light scattering (DLS), and of AuNPs (about 2 nm) via TEM images (Figure 1c). It should be noted that GA is relatively soft compared to metallic and inorganic nanoparticles, and thus the size measurement by DLS has a slight fluctuation. Figure 1d shows the absorption spectra of Au-SNPs@GA (solid lines) and bare AuNPs (dotted lines), synthesized in the presence and absence of GA respectively, by adjusting with various volumes of the 0.2% $HAuCl_4$ solution. The characteristic surface plasma resonance (SPR) band between 500 and 530 nm for Au-SNPs@GA is significantly weaker than that of bare AuNPs, indicating the formation of Au-SNPs. This observation is consistent with the previous report for supramolecularly assembled Au-SNPs.[1] The encapsulation mechanism of Au-SNPs within GA can be derived from the porous arabinogalactan (> 90%) in GA, providing a small space (pore-size 2–3 nm) to confine Au-SNPs formation.[27] To further confirm this possibility, arabinogalactan was replaced GA as a template for the preparation of Au nanocomposites, and produced similar sizes of Au-SNPs and Au-SNPs assembled structures by X-ray irradiation (Supporting Information, Figure S2).

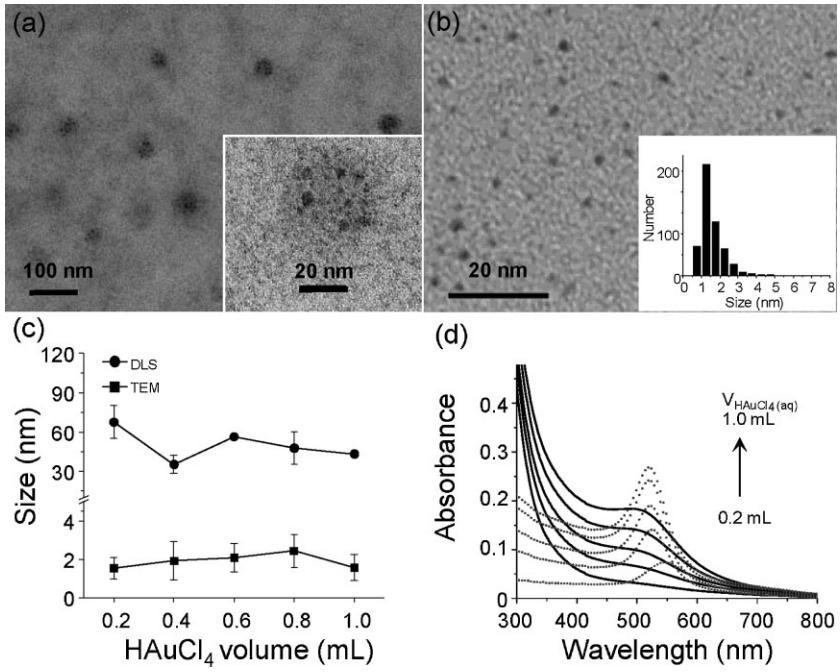

Figure 1. a) A TEM image of Au-SNPs@GA negatively stained with uranyl acetate (inset, magnified image). b) A TEM image and particle size distribution (N > 250) of Au-SNPs doped in GA. c) The size variation of Au-SNPs (square) and Au-SNPs@GA (circle) by adjusting the volume of the 0.2% $HAuCl_4$ solution against GA (40 mg mL^{-1}). d) UV-Vis spectra of Au-SNPs@GA (solid lines) and bare AuNPs (dot lines) were synthesized in the presence and absence of GA by adjusting various volumes of the 0.2% $HAuCl_4$ solution, respectively.

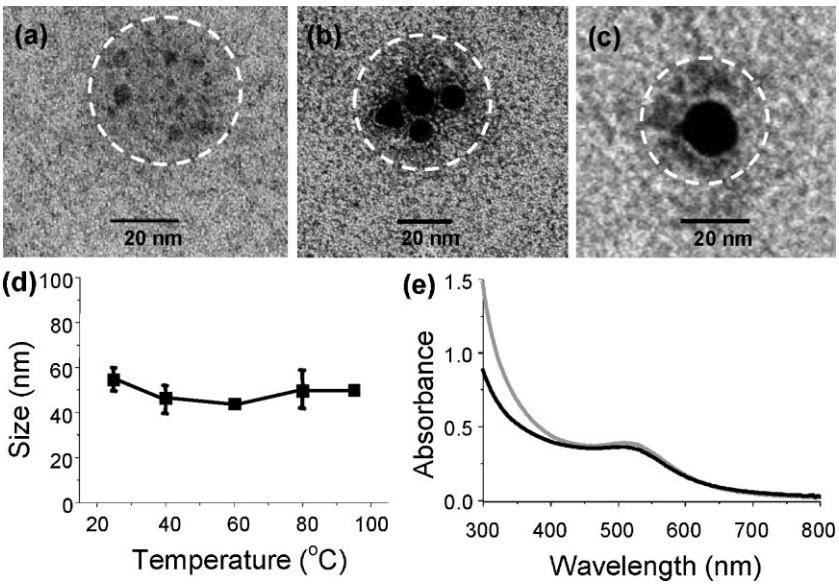

Figure 2. TEM images with negative staining of a) Synchrotron X-rays, b) $NaBH_4$, and c) microwave assisted synthesis of AuNPs in the presence of GA, respectively. d) Effect of temperature on the stability of Au-SNPs@GA. The size variation of Au-SNPs@GA in PBS was measured by DLS. e) UV-Vis spectra of our Au-SNPs@GA were measured in water (black line) and in PBS with 10% FBS (gray line), respectively.

It was also attempted to prepare the Au-SNPs@GA by using a strong chemical reagent (e.g., sodium borohydride) or microwaves, rather than only by using physical force (synchrotron X-rays), as shown in Figure 2a-c, respectively. Comparatively, reduction with sodium borohydride in the presence of GA produced slightly large sizes of Au-SNPs (3.3 ± 1.4 nm) to form Au-SNPs@GA in the fresh sample. It should be noted that the size of AuNPs became large rather than 3.3 nm as shown in Figure 2b, due to the continuous reduction of gold ions by residual sodium borohydride in the stock sample. However, in the use of microwaves instead of synchrotron X-rays, GA was used as the protecting agent for stabilizing Au-LNPs (10.9 ± 4.8 nm) in colloidal suspensions (Figure 2c). This observation was similar to those in previous reports for GA-protected Au-LNPs synthesized by different methods.[28–30] It implied that the reduction under microwaves led to the formation of Au-LNPs which cannot be confined in GA, and thus lost the AuNPs assembled structures. Consequently, GA turned out to be an effective stabilizer in preferential formation of GA-protected Au-LNPs. Synchrotron X-rays are known to efficiently generate several highly active reducing species, such as hydrogen radicals and solvated electrons,[31] which facilitate the rapid reduction of gold ions to form Au-SNPs, with their growth confined in porous GA of small size, preventing the formation of Au-LNPs and aggregations. Although chemical reduction by sodium borohydride in the presence of GA also produced AuNPs assembly, the reduction process for several hours is time-consuming. Therefore, reduction by synchrotron X-rays not only simplifies the synthesis but also avoids complicated purification, removing toxic organic solvents and chemical reagents, such as sodium borohydride.

The stability of Au-SNPs@GA was determined before conducting the following biological application. The size variations of Au-SNPs@GA in PBS were monitored by DLS at temperatures ranging from 25 to 95 °C (Figure 2d). A previous report had described that supramolecularly assembled Au-SNPs started to dissociate into small fragments at temperatures >50 °C.[1] However, our Au-SNPs@GA showed high thermal stability even at 95 °C, and a monotonous size distribution of Au-SNPs@GA was observed by DLS. TEM images with negative staining (Supporting Information, Figure S3a) show that Au-SNPs@GA kept its assembled structure after 20 min of incubation at 95 °C, with the same absorption spectra of Au-SNPs@GA at different temperatures (Supporting Information, Figure S3b). Additionally, we compared Au-SNPs@GA in water and in PBS containing a 10% FBS, using UV-vis absorption spectroscopy (Figure 2e). No significant difference in the SPR (between 500 and 530 nm) was observed for the high ionic strength solution, indicating that the Au-SNPs@GA was stable in the biological medium. Moreover, the MTT cell viability tests showed no cell toxicity (Supporting Information, Figure S4) and TNF-α expression by flow cytometry presented no immune response in bone marrow-derived dendritic cells (BMDC) (Supporting Information, Figure S5), demonstrating that the Au-SNPs@GA obtained here has good biocompatibility.

3.2. Photothermal effect of Au-SNPs@GA

The Au-SNPs@GA can be used as a new photothermal agent due to the collective heating effect related to the assembled structures.[6] In this work, we used a 532 nm green CW laser to study the laser-induced micro-bubble generation, based on the characteristic SPR band (see Figure 2e). Irradiation of the Au-SNPs@GA at 182.5 mW (NA = 0.3), viewed through a homemade microscope system (Supporting Information, Figure S6), more efficiently generated micro-bubbles, as compared to using water alone as control. In Figure S7, Supporting Information, it is demonstrated that micro-bubbles (like balloons) can rapidly form, swell and blast. It is noteworthy that unassembled Au-SNPs (about 2 nm)

colloids showed no micro-bubble generation in the previous literature.[1]

Since the bursting of micro-bubbles is known to dramatically elevate local temperatures to 374 °C (approximately the critical temperature of water),[32] the thermal disassembly of Au-SNPs@GA was also taken into consideration. According to the aforementioned high thermal stability, it was proposed that Au-SNPs@GA can resist thermal disassembly better than Au-SNPs assembly obtained by supramolecular synthetic approaches, because the structure of GA should be more rigid than the weakened supramolecular interactions. By taking the advantage of the photothermal characteristics, Au-SNPs@GA might potentially be used in multi-functionality of diagnosis through optical scattering and photoacoustic signals.[33–35]

In the following bio-related application of photothermal effect, the CW laser power was set at 99.2 mW (NA = 0.6) to ensure that no cell death can be observed before treatment with Au-SNPs@GA. Note that the Au-SNPs@GA was modified with a cell-penetration peptide (CPP) of polylysine to enhance intracellular uptake. Breast cancer cells, MDA-MB-231, were incubated with the Au-SNPs@GA for 5 h, and then changed culture medium in order to remove excess Au-SNPs@GA before laser irradiation at a fixed power (99.2 mW). Figure 3 shows that the irradiated cells underwent localized mechanical destruction within 10 s during the formation of explosive micro-bubbles. In contrast, no significant cell death was observed on the control groups, including those with no treatment (Supporting Information, Figure S8) and with treatment of Au-SNPs@GA in the absence of CPP (data not shown). The cell damage mechanism has been reported for AuNPs,[36–38] AuNPs assembly[1] and carbon nanotubes.[39,40] These results indicated that the photothermal effects of the Au-SNPs@GA were able to kill cancer cells efficiently.

3.3. Evidence for Excretion of Au-SNPs@GA

To overcome the challenge between size-dependent photothermal effects and biosafety, the bioclearance study of Au-SNPs@GA was also examined, based on in vivo pharmacokinetics and biodistribution. Figure 4a shows this pharmacokinetic study of Au-SNPs@GA. Subsequently, the raw data were fitted into a two-compartment model to present 1.49 h for half-life of distribution phase and 145 h for half-life of elimination phase, indicating that Au-SNPs@GA can be rapidly distributed into organs and more gradually removed from organs into urine and/or feces.

The biodistribution pattern in Figure 4b shows the major accumulation of Au-SNPs@GA in the liver and that the highest value is observed from four hours to six days after administration. The amount of the injected dosage (ID) was estimated at approximately 60% in the liver, which was somewhat higher and far lower than the roughly 48% for Au-SNPs and about 94% for Au-LNPs, respectively, as found in previous reports.[12] It is conceivable that the Au-SNPs@GA may strongly interact with asialoglycoprotein receptors of hepatocytes due to the arabinogalactan in GA,[41,42] resulting in accumulated increases in the liver. At day 7, the amount of Au in the liver was decreased to about 52%, implying that the Au-SNPs@GA could be removed via the kidneys and hepatobiliary systems. Indeed, the amount of total ID from urine and feces excretion at seven days was increased to about 22%.

Generally, the digested GA can only be fermented in the large intestine by microorganisms[43] and then the degraded GA forms propionate for metabolism. According

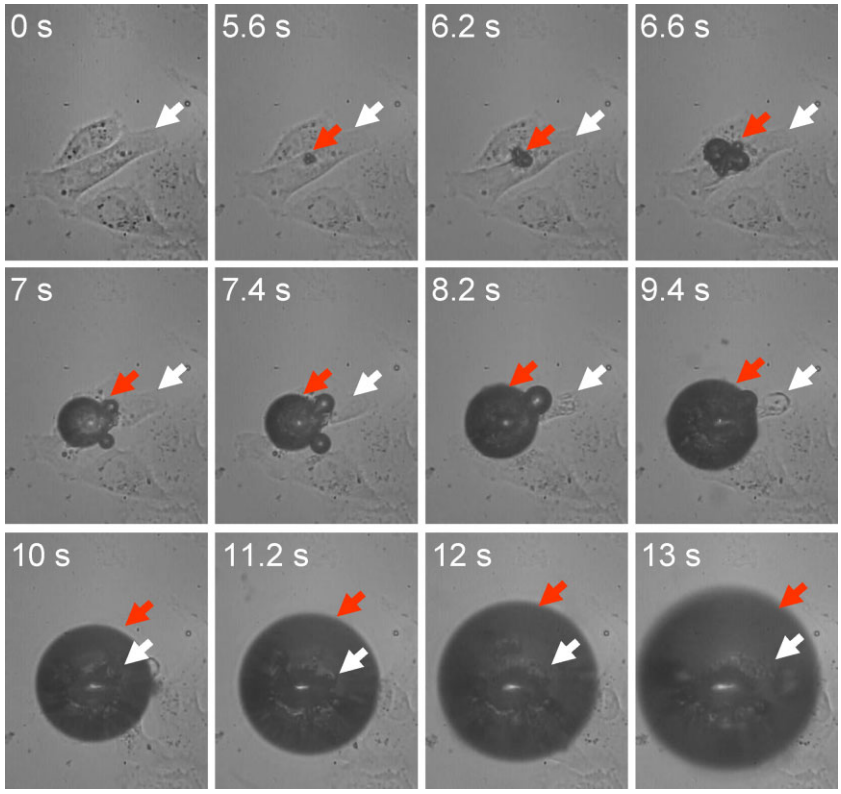

Figure 3. MDA-MB-231 cells were incubated with Au-SNPs@GA for 5 h before irradiation with a CW laser. Bright field images of micro-bubble formation (red arrows) and cell morphology (white arrows) during laser irradiation were obtained using a homemade microscope system (see Figure S6, Supporting Information) with a 40× objective lens.

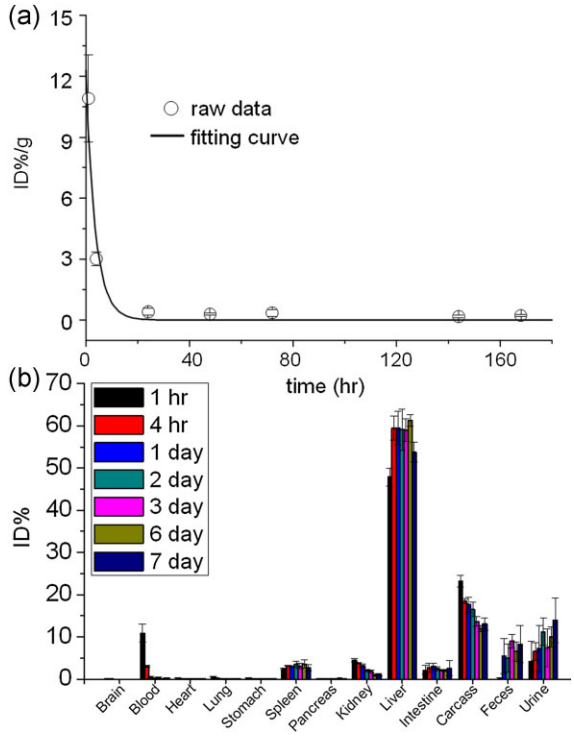

Figure 4. a) Pharmacokinetics study and b) biodistribution pattern of Au-SNPs@GA in organs, blood, carcass, feces and urine for seven days of experimentation.

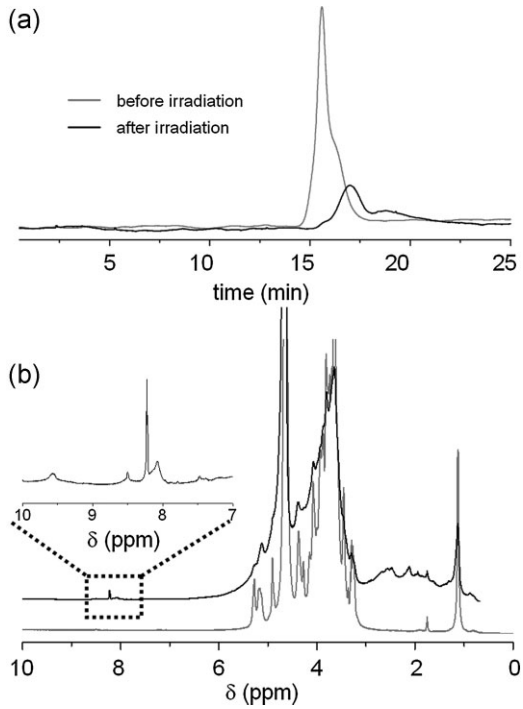

Figure 5. a) Gel permeation chromatography (GPC) and b) ^{1}H NMR spectra of GA before (gray lines) and after (black lines) irradiation with synchrotron X-rays, respectively.

to Singh's experiment,[44] the degradation of GA can occur while the GA has been partially oxidized to form hydrolytic aldehyde units. Regarding the previous GA-protected Au-LNPs (15–20 nm), their excretion evidence is controvertible[45] because noble-metal colloids with diameters compatible to renal clearance are < 8 nm.[46,47] In this work, our biodistribution studies implied that the GA may be degraded to facilitate the inside Au-SNPs toward excretion. We propose that this degradable feature may be deduced from partially oxidized GA after synchrotron X-ray irradiation. Gel-permeation chromatography (GPC) and ^{1}H NMR were used to examine the structural transformations before and after synchrotron X-ray irradiation, respectively. Figure 5a shows that the retention time of GA irradiated by synchrotron X-rays is longer than that of intact GA, indicating that the GA was degraded. In addition, the ^{1}H NMR spectrum (Figure 5b) exhibited two extra signals that were not present prior to irradiation. These extra signals appeared at about 9.6 ppm and 8.3 ppm of the NMR spectrum, and can only be observed from the X-ray irradiated GA. The two specific peaks can be assigned to aldehyde and imine groups, respectively, which may originate from the ring opening of the GA upon X-ray irradiation. Subsequently, the aldehyde moieties of GA may further react with amine of unknown proteins within GA to form imine bonds. This structural transformation of GA is well-known to hasten the excretion of polysaccharides.[44] These results illustrated that the role of synchrotron X-rays is also pivotal in making a direct impact on the excretion of our Au-SNPs@GA after intravenous injection.

4. Conclusion

In this study, we developed a simple and rapid strategy to simultaneously produce and assemble Au-SNPs to form a novel nanocomposite (Au-SNPs@GA), co-existing with GA and gold ions, upon X-ray irradiation in aqueous solutions within 5 min. GA in the precursor solution can trap gold ions for nucleation, confine the growth of Au-SNPs within its pores, prevent aggregation of Au-SNPs and result in the formation of Au-SNPs@GA. Specially, the Au-SNPs@GA exhibited strong photothermal effects, due to collective heating related to the assembled structures. Importantly, the bioclearance study demonstrated that Au-SNPs@GA may be gradually excreted by the renal and hepatobiliary system, as well as individual Au-SNPs. The simple strategy for the preparation of Au-SNPs@GA offers advantages for cancer treatment at the therapeutic level, as body-excretion can be expected to minimize toxicity concerns from long-term accumulation in vivo. In addition, this approach may be extended to other metallic colloids systems, deriving a

new class of noble-metal photothermal or other contrast agents.

Acknowledgements: C.-P. L. and F.-S.L. contributed equally to this work. This work was supported by grants from the National Health Research Institutes of Taiwan (NHRI-NM-100-PP-10) and the National Science Council (NSC-98-2113-M-400-002). Authors are also grateful to the Animal Molecular Imaging Core Facility of NHRI (NM-101-PP-04) for animal housing and radio-tracing supports, and the technical assistance from Yu-Ching Chen (NM-101-PP-12) for TEM measurements.

Received: March 26, 2013; Revised: June 6, 2013; Published online: July 16, 2013; DOI: 10.1002/mabi.201300162

Keywords: assembly; excretion; gold nanoparticles; gum Arabic; photothermal effect

[1] S. Wang, K.-J. Chen, T.-H. Wu, H. Wang, W.-Y. Lin, M. Ohashi, P.-Y. Chiou, H.-R. Tseng, *Angew. Chem. Int. Ed.* **2010**, *49*, 3777.
[2] L. Dykman, N. Khlebtsov, *Chem. Soc. Rev.* **2012**, *41*, 2256.
[3] M. P. Melancon, W. Lu, C. Li, *MRS Bull.* **2009**, *34*, 415.
[4] A. R. Lowery, A. M. Gobin, E. S. Day, K. Y. Shah, N. J. Halas, J. L. West, *Clin. Cancer Res.* **2005**, *11*, 9097s.
[5] I. H. El-Sayed, X. H. Huang, M. A. El-Sayed, *Cancer Lett.* **2006**, *239*, 129.
[6] H. H. Richardson, M. T. Carlson, P. J. Tandler, P. Hernandez, A. O. Govorov, *Nano Lett.* **2009**, *9*, 1139.
[7] K. Donaldson, V. Stone, A. Clouter, L. Renwick, W. MacNee, *Occup. Environ. Med.* **2001**, *58*, 211.
[8] G. Oberdorster, E. Oberdorster, J. Oberdorster, *Environ. Health Perspect.* **2005**, *113*, 823.
[9] X. D. Zhang, D. Wu, X. Shen, P. X. Liu, F. Y. Fan, S. J. Fan, *Biomaterials* **2012**, *33*, 4628.
[10] L. Balogh, S. S. Nigavekar, B. M. Nair, W. Lesniak, C. Zhang, L. Y. Sung, M. S. T. Kariapper, A. El-Jawahri, M. Llanes, B. Bolton, F. Mamou, W. Tan, A. Hutson, L. Minc, M. K. Khan, *Nanomed. Nanotechnol. Biol. Med.* **2007**, *3*, 281.
[11] W. H. De Jong, W. I. Hagens, P. Krystek, M. C. Burger, A. Sips, R. E. Geertsma, *Biomaterials* **2008**, *29*, 1912.
[12] M. Semmler-Behnke, W. G. Kreyling, J. Lipka, S. Fertsch, A. Wenk, S. Takenaka, G. Schmid, W. Brandau, *Small* **2008**, *4*, 2108.
[13] G. Sonavane, K. Tomoda, K. Makino, *Colloid Surf. B, Biointerfaces* **2008**, *66*, 274.
[14] S. Hirn, M. Semmler-Behnke, C. Schleh, A. Wenk, J. Lipka, M. Schäffler, S. Takenaka, W. Möller, G. Schmid, U. Simon, W. G. Kreyling, *Eur. J. Pharm. Biopharm.* **2011**, *77*, 407.
[15] C. Alric, R. Serduc, C. Mandon, J. Taleb, G. Le Duc, A. Le Meur-Herland, C. Billotey, P. Perriat, S. Roux, O. Tillement, *Gold Bull.* **2008**, *41*, 90.
[16] S. G. Jang, E. J. Kramer, C. J. Hawker, *J. Am. Chem. Soc.* **2011**, *133*, 16986.
[17] M. R. Mucalo, C. R. Bullen, M. Manley-Harris, T. M. McIntire, *J. Mater. Sci.* **2002**, *37*, 493.
[18] R. Kannan, V. Rahing, C. Cutler, R. Pandrapragada, K. K. Katti, V. Kattumuri, J. D. Robertson, S. J. Casteel, S. Jurisson, C. Smith, E. Boote, K. V. Katti, *J. Am. Chem. Soc.* **2006**, *128*, 11342.
[19] V. Kattumuri, K. Katti, S. Bhaskaran, E. J. Boote, S. W. Casteel, G. M. Fent, D. J. Robertson, M. Chandrasekhar, R. Kannan, K. V. Katti, *Small* **2007**, *3*, 333.
[20] N. Chanda, P. Kan, L. D. Watkinson, R. Shukla, A. Zambre, T. L. Carmack, H. Engelbrecht, J. R. Lever, K. Katti, G. M. Fent, S. W. Casteel, C. J. Smith, W. H. Miller, S. Jurisson, E. Boote, J. D. Robertson, C. Cutler, M. Dobrovolskaia, R. Kannan, K. V. Katti, *Nanomed. Nanotechnol. Biol. Med.* **2010**, *6*, 201.
[21] R. Kannan, A. Zambre, N. Chanda, R. Kulkarni, R. Shukla, K. Katti, A. Upendran, C. Cutler, E. Boote, K. V. Katti, *WIREs Nanomed. Nanobiotechnol.* **2012**, *4*, 42.
[22] C. C. Wu, D. H. Chen, *Gold Bull.* **2010**, *43*, 234.
[23] V. Thomas, M. Namedo, Y. M. Mohan, S. K. Bajpai, M. Bajpai, *J. Macromol. Sci., Pure Appl. Chem.* **2008**, *45*, 107.
[24] A. Biffis, N. Orlandi, B. Corain, *Adv. Mater.* **2003**, *15*, 1551.
[25] Y. Wang, R. Yan, J. Z. Zhang, W. Q. Zhang, *J. Mol. Catal. A: Chem.* **2010**, *317*, 81.
[26] C.-H. Wang, C.-C. Chien, Y.-L. Yu, C.-J. Liu, C.-F. Lee, C.-H. Chen, Y. Hwu, C.-S. Yang, J.-H. Je, G. Margaritondo, *J. Synchrot. Radiat.* **2007**, *14*, 477.
[27] C. Sanchez, C. Schmitt, E. Kolodziejczyk, A. Lapp, C. Gaillard, D. Renard, *Biophys. J.* **2008**, *94*, 629.
[28] N. R. Jana, L. Gearheart, C. J. Murphy, *Langmuir* **2001**, *17*, 6782.
[29] M. Tsuji, M. Hashimoto, Y. Nishizawa, M. Kubokawa, T. Tsuji, *Chem. Eur. J.* **2005**, *11*, 440.
[30] R. Harpeness, A. Gedanken, *Langmuir* **2004**, *20*, 3431.
[31] E. Gachard, H. Remita, J. Khatouri, B. Keita, L. Nadjo, A. Jacqueline Belloni, *New J. Chem.* **1998**, *22*, 1257.
[32] V. Kotaidis, A. Plech, *Appl. Phys. Lett.* **2005**, *87*, 213102.
[33] E. Y. Lukianova-Hleb, Y. Hu, R. A. Drezek, J. H. Hafner, D. O. Lapotko, *Nanomed. Nanotechnol. Biol. Med.* **2008**, *3*, 797.
[34] E. Y. Lukianova-Hleb, D. O. Lapotko, *Nano Lett.* **2009**, *9*, 2160.
[35] D. S. Wagner, N. A. Delk, E. Y. Lukianova-Hleb, J. H. Hafner, M. C. Farach-Carson, D. O. Lapotko, *Biomaterials* **2010**, *31*, 7567.
[36] E. Y. Lukianova-Hleb, J. H. Hafner, J. N. Myers, E. Y. Hanna, B. C. Rostro, S. A. Zhdanok, D. O. Lapotko, *Nanomed. Nanotechnol. Biol. Med.* **2008**, *3*, 647.
[37] T. H. Wu, S. Kalim, C. Callahan, M. A. Teitell, P. Y. Chiou, *Opt. Express* **2010**, *18*, 938.
[38] D. O. Lapotko, E. Y. Lukianova-Hleb, A. A. Oraevsky, *Lasers Surg. Med.* **2006**, *38*, 631.
[39] B. Kang, D. C. Yu, Y. D. Dai, S. Q. Chang, D. Chen, Y. T. Ding, *Small* **2009**, *5*, 1292.
[40] F. F. Zhou, S. N. Wu, Y. Yuan, W. R. Chen, D. Xing, *Small* **2012**, *8*, 1543.
[41] E. V. Groman, P. M. Enriquez, C. Jung, L. Josephson, *Bioconjugate Chem.* **1994**, *5*, 547.
[42] Y. Kaneo, T. Ueno, T. Tanaka, H. Iwase, Y. Yamaguchi, T. Uemura, *Int. J. Pharm.* **2000**, *201*, 59.
[43] B. H. Ali, A. Ziada, G. Blunden, *Food Chem. Toxicol.* **2009**, *47*, 1.
[44] M. Singh, A. R. Ray, A. P. Vasudevan, *Biomaterials* **1982**, *3*, 16.
[45] G. M. Fent, S. W. Casteel, D. Y. Kim, R. Kannan, K. Katti, N. Chanda, K. Katti, *Nanomed. Nanotechnol. Biol. Med.* **2009**, *5*, 128.
[46] S. Mitragotri, J. Lahann, *Nat. Mater.* **2009**, *8*, 15.
[47] A. E. Nel, L. Madler, D. Velegol, T. Xia, E. M. V. Hoek, P. Somasundaran, F. Klaessig, V. Castranova, M. Thompson, *Nat. Mater.* **2009**, *8*, 543.